Nonlinear Simulations of Fishbone Instability and Sawteeth in Tokamaks and Spherical Torus

G. Y. Fu, J. A. Breslau, W. Park, S. C. Jardin, J. Chen
Princeton Plasma Physics Laboratory, Princeton, NJ 08543, U.S.A.

e-mail: fu@pppl.gov

Abstract

We report new results of self-consistent nonlinear simulations of fishbone instability and sawtooth oscillations obtained using the extended MHD code M3D. Hybrid simulations of energetic particle-driven fishbone instability in a circular tokamak show dynamic mode saturation as the particle distribution is flattened and mode frequency is reduced strongly. MHD nonlinearity reduces the mode saturation level. Resistive MHD simulations of the CDX-U spherical torus show repeated sawtooth cycles with calculated periodicity consistent with the experimental observation. The two-fluids simulations show that the induced sheared plasma rotation suppresses the island growth so that the magnetic field no longer passes through a stochastic state as observed in the MHD simulations. Resistive MHD simulations of sawtooth crashes in the TEXTOR tokamak show that the localization effect of reconnection is rather small. Even when the pressure in the core is flattened due to stochasticity in a nonlinear state, the complete reconnection process still tends to proceed with q(0) rises above one.

1 Introduction

Understanding of nonlinear behavior of $m = 1$ mode in tokamaks is of fundamental importance for burning plasmas. In this paper, we present recent results on energetic particle-driven fishbone instability and sawtooth oscillations simulated by the global nonlinear extended MHD code M3D[1].

The M3D code contains multiple levels of physics including resistive MHD, two fluids[2], and particle/MHD hybrid[1]. The resistive and two fluids models are used to simulate sawtooth oscillations, whereas the hybrid model is used to investigate the nonlinear dynamics of fishbone instability. The code solves the extended MHD equations as an initial value problem with both fluid and particle nonlinearity in 3D geometry. It uses finite elements in poloidal planes and finite difference in toroidal direction. It runs on massively parallel super-computers by using MPI. The code has been recently used to simulate sawtooth oscillations[3], energetic-particle-driven fishbone[4] and Alfven instability[5], alpha particle stabilization of internal kink mode in ITER[4], nonlinear saturation of internal kink mode in NSTX[6], two-fluids stabilization of MHD modes in stellarators[7], and nonlinear evolution of edge localized modes (ELM) in tokamaks[8].

2 Fishbone instability

The fishbone instability was first discovered in the PDX tokamak. The name "fishbone" came from the characteristic shape of the magnetic signal from the Mirnov coils. It is basically an $(n, m) = (1, 1)$ internal kink mode destabilized by energetic trapped particles

via precessional resonance. Here we use the M3D hybrid code to study the excitation and nonlinear evolution of the fishbone instability driven by energetic particles. In particular, we investigate the nonlinear dynamics of the instability self-consistently[4].

We start with linear simulations. We consider a sequence of circular tokamak equilibria with increasing energetic particle pressure. The plasma parameters are: aspect ratio $R/a = 2.763$, total central beta $\beta(0) = 8\%$, central and edge safety factor $q(0) = 0.9$, $q(a) = 2.5$. The energetic particle distribution is an isotropic slowing-down one with $\rho_h/a = 0.05$ and $v_0/v_A = 1$. Figure 1**a** plots the fishbone growth rate and mode frequency versus energetic particle beta $\beta_h(0)$ from three cases: A) $\beta_h(0) = 2.6\%$, B) $\beta_h(0) = 4.3\%$, and C) $\beta_h(0) = 5.7\%$. The plasma thermal beta is very small, with $\beta_h/\beta_{total} \sim 0.9$ for all these cases. Figure 1**b** shows the velocity stream function U of the linear eigenmode for case B. We observe that the eigenmode structure is mainly a $(1,1)$ mode as expected. We also observe in Fig. 1**a** that the growth rate increases approximately linearly as a function of $\beta_h(0)$ while the mode frequency varies slightly about $\omega \sim 0.04$. This frequency is comparable to the nominal energetic particle precessional frequency $\omega_d/\omega_A \sim \frac{1}{2}k_\theta\rho_h v_h/v_A \sim 0.05$. These results are consistent with analytic results for the fishbone instability.

We now turn to nonlinear simulation results. We first focus on the particle nonlinearity by imposing a linear MHD response from the thermal species. Figure 2**a** shows the nonlinear evolution of U_{cos} (the $cos\phi$ component of U) for case A, B and C. We observe that the mode first grows linearly and then begins to saturate after a few oscillations. The initial saturation amplitude scales as $U_{amp} \sim \gamma^2$. It is interesting to note that after the initial saturation, the mode amplitude can oscillate (case A with smallest growth rate), or decay slowly (case B) or decay rapidly (case C with largest linear growth rate). We also observe that the frequency of the mode chirps down significantly as the mode oscillation period increases for all these cases. We observe up to a factor of two reduction in mode frequency at the end the simulation runs.

We now investigate the physical mechanism for saturation and mode frequency chirping. Figure 2**b** shows the evolution of the energetic particle distribution at particle speed $v/v_A \sim 0.8$ and pitch angle $\Lambda = \mu B_0/E \sim 1.0$. Note that the horizontal axis P_ϕ corresponds to a radial variable ranging from -0.42 at the center of plasma to 0 at the plasma edge. We observe that the distribution becomes flattened starting from $t \sim 500$ when the mode frequency begins to chirp down rapidly. Furthermore, the flattening region widens clearly from this time. Notice that the shoulder of the flattening region moves out radially in time. Since the instability is driven by df/dP_ϕ, the initial saturation is caused by the nonlinear flattening of the distribution. On the other hand, the frequency chirping can be explained by the movement of the shoulder in the distribution function. In the nonlinear evolution, we expect the mode frequency evolves according to the distribution evolution in order to maximize instability drive. In particular, we expect that the maximum drive comes from the steep gradient region just outside the shoulder region. Since the precession drift frequency of trapped particles at fixed energy and pitch angle is smaller for larger P_ϕ (or larger radius), the mode frequency needs to decrease in time as the steep gradient region moves out radially in order to satisfy the resonant condition $\omega = \omega_d$ and tap the free energy associated with the df/dP_ϕ.

So far, we have neglected the MHD nonlinearity in the nonlinear simulations. We have also carried out simulations with both particle nonlinearity and MHD nonlinearity. The results show that the MHD nonlinearity reduces the initial saturation level. However, the MHD nonlinearity does not enhance the initial mode growth in contrast to the results of Odblom et al.[9]. In the work of Odblom et al., the MHD nonlinear enhancement of the initial mode growth was found near marginal stability when the linear mode had a double layer radial structure around the q=1 surface. In this work, however, the linear mode has

a single layer structure around the q=1 surface due to finite numerical viscosity.

Finally it should be pointed out that our results for the nonlinear fishbone is qualitatively similar to the hole-clump theory of the bump-in-tail instability by Berk *et al.*[10]. In particular, the nonlinear frequency evolution approximately scales as $\delta f \sim \sqrt{t}$ as found analytically by their theory. Of course, quantitative agreement is not expected since our model is much more comprehensive and self-consistent.

3   Sawtooth Oscillations in CDX-U

The resistive internal kink instability in tokamaks leads to the phenomenon of the sawtooth crash[11], which mixes plasma from the core and outer regions, cooling the center. It is therefore desirable to develop a model of the triggering and consequences of such events that provides a quantitative predictive capability so that they can be avoided or controlled. Analytic theories and quasi-empirical theory-based models such as that of Porcelli[12] provide a good starting point, but more fundamental numerical models stand a better chance of giving accurate numbers for particular discharges in particular physical devices and for testing and optimizing various control techniques. Resistive MHD phenomena involving magnetic reconnection, such as the sawtooth crash, are associated with thin sheets of high current density whose thickness scales as Lundquist number $S^{-1/2}$. In large, hot tokamak experiments S is typically of the order of 10^8 or higher, which would result in current sheets too thin to be practically resolved in a calculation that makes use of a partially explicit time advance. In contrast, smaller, colder tokamaks with S of 10^5 or lower may have current sheets thick enough to be resolved in a long calculation, and so are better candidates for realistic MHD physics simulation on present-day computers. The resistive MHD model gives a reasonable description of magnetic reconnection in these devices, although there will be some quantitative differences when the more complete extended MHD model is used. The Current Drive Experiment Upgrade (CDX-U)[13] is a small, low-aspect ratio university-scale tokamak at the Princeton Plasma Physics Laboratory. While its discharges are much colder and briefer than those in larger experiments, it is reasonably well-diagnosed, and exhibits the same MHD instabilities that are of interest in reactor-relevant devices. In particular, it has a sawtooth regime with an easily characterizable period of approximately $125\mu s$. With $S \sim 10^4$, it is therefore an ideal candidate for modeling with M3D.

The study[3] begins with a sequence of equilibria that occur as time slices from a reconstruction of a typical CDX-U discharge using the 2D (axisymmetric) transport-timescale code TSC[14]. During the course of the discharge, the plasma current increases sufficiently to cause central safety factor $q(0)$ to fall below unity, the condition for instability of the sawtooth mode. The reference case for the simulations described in the rest of this paper is one for which $q(0)$ has dropped to 0.92, increasing monotonically outward, with the $q = 1$ surface approximately a third of the way out from the axis. A description of this equilibrium state is then imported into M3D as an initial condition. The initial resistivity is taken to be the Spitzer value based on the initial temperature profile, which gives a peak S of 1.94×10^4, with the minimum value constrained to be no smaller than 1.94×10^2. The resistivity is not evolved in time. The viscosity is set to ten times the resistivity at the peak location and is constant in space and time. The first task was to run the M3D code in its linear mode in order to determine the eigenmodes and linear growth rates of the starting equilibrium for the first few toroidal mode numbers. From this it was determined that the equilibrium is unstable to an $m = 1, n = 1$ mode consistent with the sawtooth model, with a normalized linear growth rate of $\gamma\tau_A = 8.61 \times 10^{-3}$. The remaining studies are full nonlinear runs of the code, initialized by superimposing this

eigenmode on the equilibrium state at an amplitude such that the maximum B_p in the perturbation is 10^{-4} of the maximum B_T in the equilibrium. At various mesh resolutions, the plasma is allowed to evolve in the presence of volumetric source terms that tend to restore the current density and temperature to their equilibrium values. The two highest-n resolvable toroidal modes are filtered out to avoid aliasing problems; the others are kept and couple to each other in a fully nonlinear way. The behavior of the current and temperature profiles and of the field topology are closely monitored for indications of $m = 1$ activity as the equations are solved out to several predicted sawtooth periods. As shown in Fig. 3, this nonlinear run begins with a long phase of essentially linear behavior during which the $n = 1$ mode grows at the linearly predicted rate, while nonlinearly coupling to and destabilizing higher n modes.

The sequence of Poincaré plots in Fig. 4 shows the evolution of the magnetic flux surfaces during a typical sawtooth cycle. The nonlinear $m = 1$, $n = 1$ mode results in a complete sawtooth crash, with formation of a new magnetic axis, and reconnection of the original one, as in the Kadomtsev model[15]. Because the $n = 1$ mode and the nonlinearly driven higher-n modes also have higher m components at rational surfaces with $q > 1$, the $(1, 1)$ island merging coincides with the growth and overlap of other island chains at larger minor radii, resulting in general stochasticity after the "crash". As a current source term gradually drives the central safety factor back below unity (and a temperature source reheats the cooled core region), the stochastic regions heal and again become good flux surfaces. The process then repeats. The cycle time of $395\tau_A$ is equivalent to about $100\mu s$, in reasonably good agreement with observations.

In order to assess numerical convergence, the nonlinear study was repeated with the same poloidal resolution but with twice the toroidal resolution, allowing modes up to n=22 to be resolved. The behavior of the higher-resolution run, however, was qualitatively different from that of the initial one. The initial crash happened sooner and with greater violence, and subsequent crashes followed with a shorter period but with diminishing energy. This failure to converge with more planes appears to be caused by the presence of large amounts of energy in the additional modes. We are performing additional studies to determine whether these short-wavelength modes are physical or are artifacts of converging in only one dimension or of the simplified resistive MHD model.

The nonlinear phase of the study was repeated with the ion diamagnetic $(\omega_i^\star)$ term from the two-fluid model turned on. The effect was modest, and the behavior of the plasma was qualitatively similar to the resistive MHD result. Notable differences include an overall toroidal rotation of the plasma, small oscillations in the energies of the higher-n modes during the early nonlinear phase, and a 4% increase in the sawtooth period. Additionally, growth of the secondary islands was suppressed, presumably by the shear in the plasma rotation, with the result that the magnetic field did not become stochastic after the first crash. Reconnection of the $(1, 1)$ island was incomplete during the second crash and appeared to reverse direction toward the end. Further convergence studies are underway to confirm these results.

In conclusion, in a series of high-resolution, massively parallel nonlinear MHD runs, the sawtooth cycle in the CDX tokamak has been successfully tracked with the M3D code in a series of high-resolution, massively parallel nonlinear MHD runs. The lower-resolution case showed good agreement with the observed sawtooth period (though not with the observed crash time), but the higher-resolution check failed to agree with this period. It is likely that still higher resolutions, as well as greater fidelity to the physics of the actual experiment, will be required to produce good quantitative agreement. Areas for improvement include the use of extended (two-fluid) MHD terms which are likely to give faster reconnection and to preferentially damp the higher-n modes; and the use of ohmic heating and current drive rather than the volume source terms now in use for these

quantities, which do not have direct analogues in the device. Better transport models, including an evolving resistivity profile and a perpendicular heat transport profile with much smaller interior values, will also be required.

4 Simulation of the Sawteeth in TEXTOR

A long standing puzzle in tokamak research is that some experimental measurements show that the central q value consistently does not rise above one, after a sawtooth crash[16], while theory and simulation generally show $q(0)$ rise above one after a typical crash, as M3D simulations have also shown over the years. There are, however, at least two theories trying to explain $q(0)$ staying below one: various modeling of magnetic field line stochasticity and localized reconnection picture[17]. One can expect some similarity between these two theories because the main effect of a localized reconnection is to produce stochasticity. (Since magnetic topology is a global character which cannot be specific to a toroidal plane, a toroidally varying reconnection produces stochasticity.)

To clarify this situation, we have performed MHD and two-fluid simulations using M3D, specifically for TEXTOR geometry and parameters. The result shows that the localized reconnection and thus stochasticity is not significant, and the magnetic topology goes through the usual complete reconnection and $q(0)$ rises above one. Nevertheless, to further ascertain this result, we numerically exaggerated the localization of reconnection by making the resistivity a strong function of the sheet current strength, which resulted in a complete stochasticity of the "hot spot" as shown in Fig. 5(a). This gives a minor decrease of temperature compared to the previous case (minor because the crash time is fast), while the current evolution (and to a lesser extent the temperature evolution) proceeds similarly as in the previous case and $q(0)$ rises above one after the crash. To ascertain this result still further, the temperature is numerically flattened as shown in Fig. 5(b) as the hot spot becomes stochastic. This still gave a current evolution similar as before: $q(0)$ rising above one when flux surfaces recover after the crash as shown in Fig. 5(c). This run was done using MHD model plus ion diamagnetic effects and electron parallel thermal conduction.

References

[1] W. Park, E.V. Belova, G.Y. Fu et al., Phys. Plasmas **6** 1796 (1999).

[2] L.E. Sugiyama and W Park, **7**, 4644 (2000).

[3] J.A. Breslau, W. Park and S.C. Jardin, J. Phys.: Conf. Ser. 46, 97-101 (2006).

[4] G.Y. Fu et al., Phys. Plasmas **13**, 052517 (2006).

[5] G.Y. Fu et al., The 20th IAEA Fusion Energy Conference, 2004, paper TH/P4-38.

[6] W. Park et al.,, The 19th IAEA Fusion Energy Conference, paper TH/5-1

[7] H.R. Strauss, L.E. Sugiyama, G.Y. Fu et al., Nucl. Fusion **44**, 1008 (2004).

[8] H.R. Strauss et al., The 21st IAEA Fusion Energy Conference, paper TH/P8-6.

[9] A. Odblom, B.N. Breizman, S.E. Sharapov, T.C. Hender and V. P. Pastukhov, Phys. Plasmas **9**, 155 (2001).

[10] H.L. Berk, B.N. Breizman, and J. Candy, M. Pekker and N.V. Petviashili, Phys. Plasmas **6**, 3102 (1999).

[11] von Goeler S, Stodiek W and Sauthoff N Phys. Rev. Lett. **33**, 1201 (1974).

[12] Porcelli F, Boucher D and Rosenbluth M, Plasma Phys.and Contr. Fusion **38**, 2163 (1996).

[13] Menard J, Majeski R, Kaita R, Ono M, Munsat T, Stutman D, Finkenthal M, Choe W, Hwang YS, Petrov Y, Gusev G and Seki T, Phys. Plasmas **6**, 2002 (1996).

[14] Jardin S, Pomphrey N and DeLucia J L, J. Comp. Phys. **66**, 481 (1986).

[15] Kadomtsev B B, Sov. J. Plasma Phys. **1**, 389 (1975).

[16] H. Soltwisch, Rev. Sci. Instrum. **59**, 1599 (1989).

[17] Y. Nagayama, et al., Phys. Plasmas **3**, 1647 (1996).
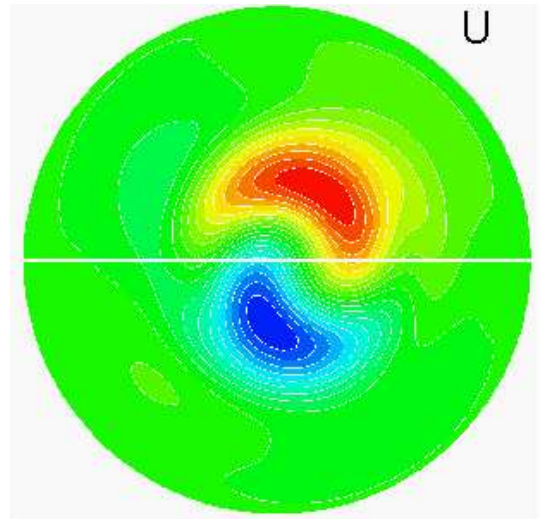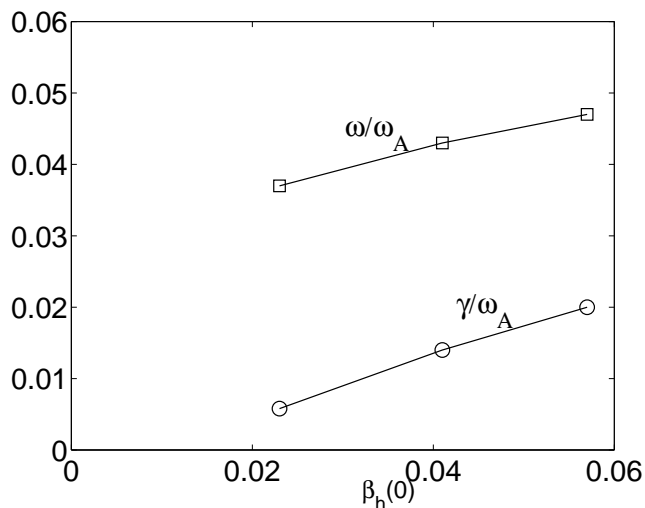
Figure 1: **a.** The fishbone mode frequency and growth rate vs energetic particle beta (left); **b.** The contours of the fishbone linear eigenmode for velocity stream function U (right).
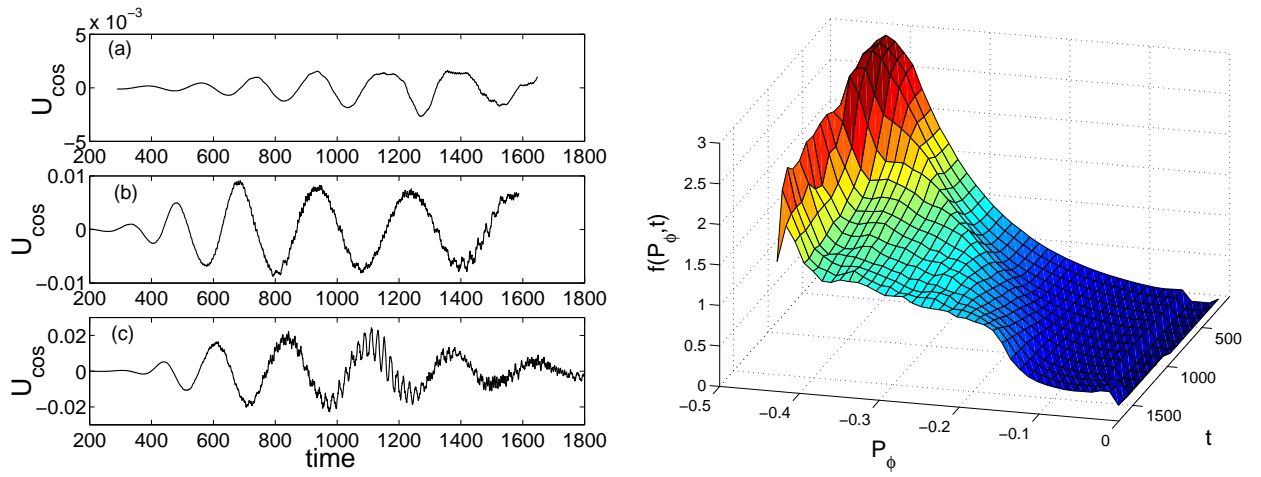
Figure 2: **a.** Nonlinear evolution of the *cos* component of U for case A, B and C (left); **b.** The trapped particle distribution function vs time at $v/v_A = 0.8$ and $\Lambda = 1.0$ (right).
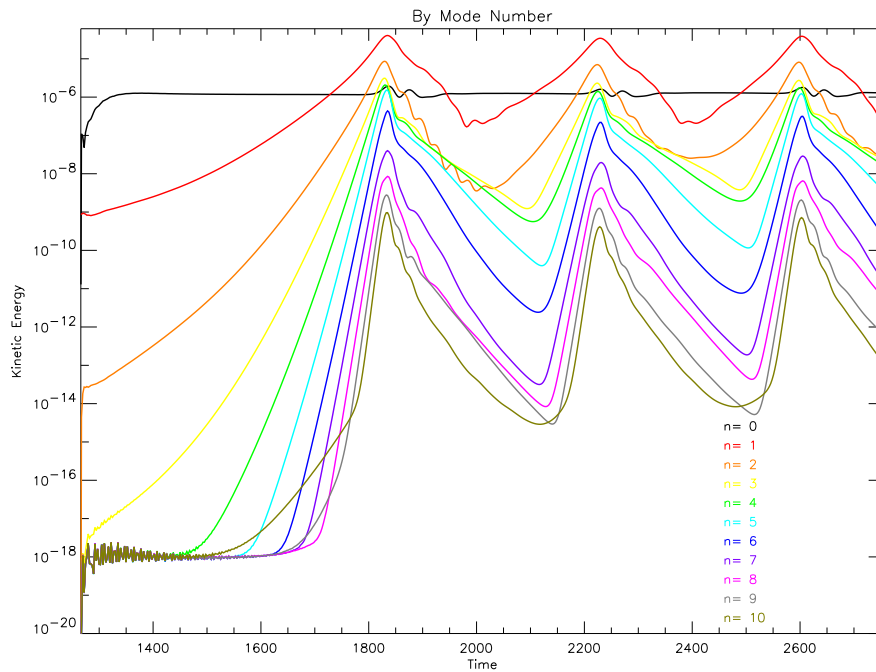
Figure 3: Total kinetic energy by mode number during nonlinear sawtooth runs with 10 toroidal modes retained.
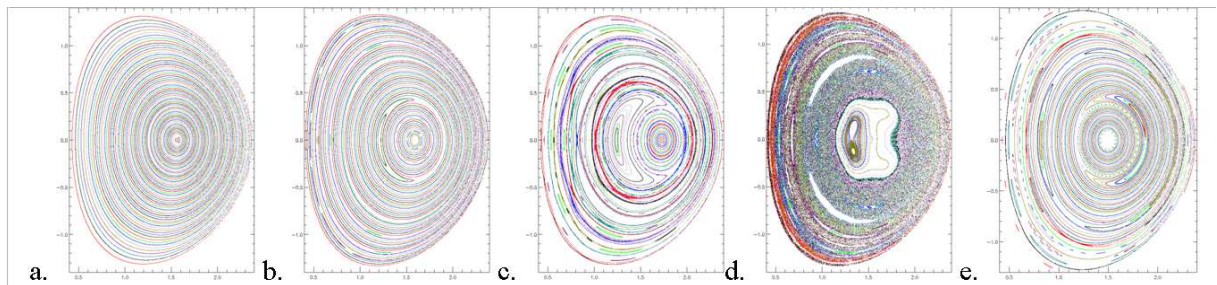
Figure 4: Poincaré sections showing intersection of magnetic surfaces with the $\phi = 0$ plane at several time slices during the course of the nonlinear 10-mode CDX run depicted in Fig. 3. **a.** Initial State, $t = 1266.17$. **b.** Island growing, $t = 1660.70$. **c.** Nonlinear phase, $t = 1795.61$. **d.** After first crash, $t = 1839.86$. **e.** Flux surfaces recovered, $t = 2094.08$.
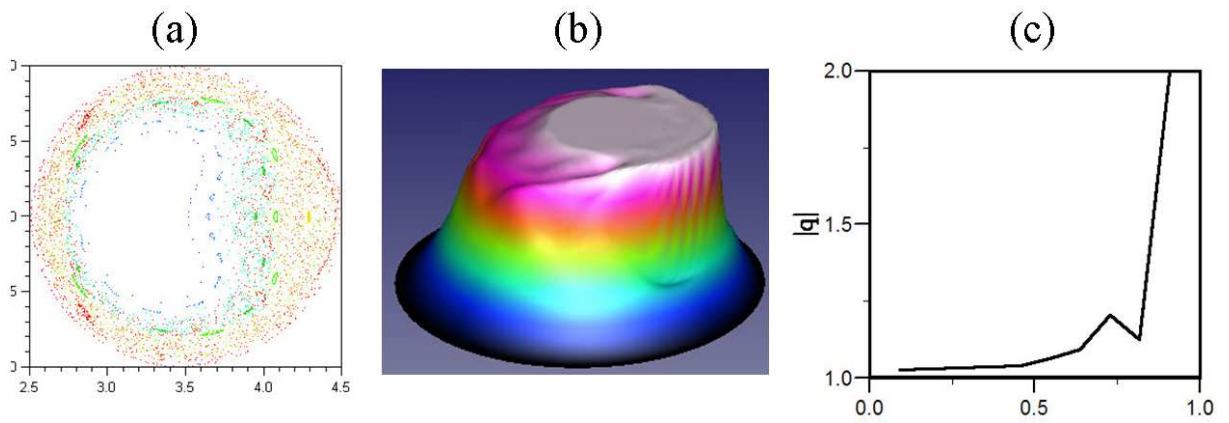
Figure 5: Results of M3D simulations of sawtooth crash in the TEXTOR tokamak: (a) complete stochasticity of the "hot spot" induced by a localized resistivity; (b) an artificially flattened temperature profile; (c) q profile after sawtooth crash with the temperature profile in (b).